Atmos. Chem. Phys. Discuss., doi:10.5194/acp-2017-161, 2017
Manuscript under review for journal Atmos. Chem. Phys.
Discussion started: 29 March 2017

Atmospheric Chemistry and Physics Discussions
Open Access

OMI measured increasing SO_2 emissions due to energy industry expansion and relocation in Northwestern China

Authors:
Zaili Ling[1], Tao Huang[1,*], Yuan Zhao[1], Jixiang Li[1], Xiaodong Zhang[1], Jinxiang Wang[1], Lulu Lian[1], Xiaoxuan Mao[1], Hong Gao[1], Jianmin Ma[1,2,3,*]

Affiliations:
[1]Key Laboratory for Environmental Pollution Prediction and Control, Gansu Province, College of Earth and Environmental Sciences, Lanzhou University, Lanzhou 730000, P. R. China
[2]Laboratory for Earth Surface Processes, College of Urban and Environmental Sciences, Peking University, Beijing, 100871, China
[3]CAS Center for Excellence in Tibetan Plateau Earth Sciences, Chinese Academy of Sciences, Beijing, 100101, China

Corresponding author: Jianmin Ma, Tao Huang
College of Earth and Environmental Sciences, Lanzhou University, 222, Tianshui South Road, Lanzhou 730000, China

Email: jianminma@lzu.edu.cn; huangt@lzu.edu.cn

Atmos. Chem. Phys. Discuss., doi:10.5194/acp-2017-161, 2017
Manuscript under review for journal Atmos. Chem. Phys.
Discussion started: 29 March 2017

Abstract

The rapid economy growth makes China the largest energy consumer and sulphur dioxide (SO_2) emitter in the world. In this study, we estimated the trends and step changes in the planetary boundary layer (PBL) vertical column density (VCD) of SO_2 from 2005 to 2015 over China measured by the Ozone Monitoring Instrument (OMI). We show that these trends and step change years coincide with the effective date and period of the national strategy for energy development and relocation in northwestern China and the regulations in the reduction of SO_2 emissions. Under the national regulations in the reduction SO_2 emissions in eastern and southern China, SO_2 VCD in the Pearl River Delta (PRD) of southern China exhibited the largest decline during 2005-2015 at a rate of -7% yr^{-1}, followed by the North China Plain (NCP) (-6.7% yr^{-1}), Sichuan Basin (-6.3% yr^{-1}), and Yangtze River Delta (YRD) (-6% yr^{-1}), respectively. The Mann–Kendall (MK) test reveals the step change points of declining SO_2 VCD in 2009 for the PRD and 2012-2013 for eastern China responding to the implementation of SO_2 control regulation in these regions. In contrast, the MK test and regression analysis also revealed increasing trends of SO_2 VCD in northwestern China, particularly for several "hot spots" featured by growing SO_2 VCD in those large-scale energy industry parks in northwestern China. The enhanced SO_2 VCD is potentially attributable to increasing SO_2 emissions due to the development of large-scale energy industry bases in energy-abundant northwestern China under the national strategy for the energy safety of China in the 21st century. We show that these large-scale energy industry bases could overwhelm the trends and changes in provincial total SO_2

Atmos. Chem. Phys. Discuss., doi:10.5194/acp-2017-161, 2017
Manuscript under review for journal Atmos. Chem. Phys.
Discussion started: 29 March 2017

emissions in northwestern China and contributed increasingly to the national total SO_2 emission in China. Given that northwestern China is more ecologically fragile and uniquely susceptible to atmospheric pollution as compared with the rest of China, increasing SO_2 emissions in this part of China should not be overlooked and merit scientific research.

1. Introduction

Sulfur dioxide (SO_2) is one of the criteria air pollutants emitted from both anthropogenic and natural sources. The combustions of sulfur-containing fuels, such as coal and oil, are the primary anthropogenic emitters, which contributed to the half of total SO_2 emissions (Smith et al., 2011; Lu et al., 2010; Stevenson et al., 2003; Whelpdale et al., 1996).With the rapid economic growth in the past decades, China has become the world's largest energy consumer accounting for 23% of global energy consumption in 2015 (BIEE, 2016). Coal has been a dominating energy source in China and accounted for 70% of total energy consumption in 2010 (Kanada et al., 2013). The huge demand to coal and its high sulfur content make China the largest SO_2 emission source in the world (Krotkov et al., 2016; Su et al., 2011), which also accounted for two-third of Asia's total SO_2 emission (Ohara et al., 2007). From 2000 to 2006, the total SO_2 emission in China increased by 53% at an annual growth rate of 7.3% (Lu et al., 2010). To reduce SO_2 emission, from 2005 onward the Chinese government has issued and implemented a series of regulations, strategies, and SO_2 control measures, leading to a drastic decrease of SO_2 emission, particularly in eastern

Atmos. Chem. Phys. Discuss., doi:10.5194/acp-2017-161, 2017
Manuscript under review for journal Atmos. Chem. Phys.
Discussion started: 29 March 2017

and southern China (Lu et al., 2011; Li et al., 2010).

Recently, two research groups led by NASA (National Aeronautics and Space Administration) and Lanzhou University of China published almost simultaneously the temporal and spatial trends of SO_2 in China from 2005 to 2015 using the OMI retrieved SO_2 PBL column density after the OMI is lunched for 11 years (Krotkov et al., 2016; Shen et al., 2016). The results reported by the two groups revealed widespread decline of SO_2 in eastern China for the past decade. Shen et al noticed, however, that, in contrast to dramatic decreasing SO_2 emissions in densely populated and industrialized eastern and southern China, the OMI measured SO_2 in northwestern China appeared not showing a decreasing trend. This is likely resulted from the energy industry relocation and development in energy-abundant northwestern China in the past decades under the national strategy for China's energy development and safety during the 21st century. Concern is raised for the potential impact of SO_2 emissions on the ecological environment and health risk in northwestern China because high SO_2 emissions could otherwise damage the rigorous ecological environment in this part of China, featured by very low precipitation and sparse vegetation coverage which reduce considerably the atmospheric removal of air pollutants (Ma and Xu, 2017).

To assess and evaluate the risks of the ecological environment and public to the growing SO_2 emissions in northwestern China, it is necessary to investigate the spatiotemporal distributions of SO_2 concentrations and emissions. However, the ground measurements of ambient SO_2 are scarce temporally and spatially in China, and often subject to large errors and uncertainties. Owing to the rapid progresses in the remote sensing techniques, satellite retrieval of air pollutants has become a powerful tool in the assessment of emissions and spatiotemporal distributions of air pollutants. In recent several years, OMI (Dutch Space, Leiden, The Netherlands, embedded on Aura satellite) retrieved SO_2 column concentrations have been increasingly applied to elucidate the spatiotemporal variation of global and regional SO_2 levels and its emissions from large point sources, and evaluate the effectiveness of SO_2 control policies and measures (Krotkov et al., 2016; McLinden et al., 2015, 2016; Ialongo et al., 2015; Fioletov et al., 2015, 2016; Wang et al., 2015; Li et al., 2010). The decadal operation of the OMI provides the relatively long-term SO_2 time series data with high spatial resolution which are particular useful for assessing the changes and trends in SO_2 emissions induced by national regulations and strategies. The present study aims to (1) assess the spatiotemporal variations of SO_2 and its trend under the national strategy for energy industry development in northwestern China by making use of the OMI-measured SO_2 data during 2005-2015; (2) to further examine the usefulness of the satellite remote sensing of air quality.

2 Data and methods

2.1 Satellite data

We collected the level 3 OMI daily planetary boundary layer (PBL) SO_2 vertical column density (VCD) data in Dobson units (1 DU=2.69×10^{16} molecules cm^{-2}) produced by the principal component analysis (PCA) algorithm (Li et al., 2013). The spatial resolution is 0.25°×0.25° latitude/ longitude, available at Goddard Earth Sciences Data and Information Services Center (http://disc.sci.gsfc.nasa.gov/Aura/data-holdings/OMI/omso2_v003.shtml). This algorithm yields one-step SO_2 VCD. However, as Fioletov et al (2016) noted, the PCA retrieved SO_2 VCD was virtually derived by adoption of an effective air mass factor (AMF) of 0.36 which is best applicable in the summertime in the eastern United States (US). The algorithm may cause systematic errors if anthropogenic emission sources are located in different latitudes and under complex topographic and underlying surface conditions. For instance, Wang (2014) has shown that AMF≈0.57 in eastern China. In the present study, we have adopted the AMFs values in China provided by Fioletov et al (2016) to adjust OMI measured VCD in the estimation of the SO_2 emission burden of major point sources in northwestern China.

2.2 SO_2 monitoring, emission, and socioeconomic data

Figure 1 is a China map which highlights 6 provinces in northwestern China, including Shaanxi, Gansu, Qinghai, Ningxia, Xinjiang, and Inner Mongolia. Traditionally, Inner Mongolia is not classified as a northwestern province in China. Given that the most energy resources in Inner Mongolia are located in its western part of this province (Fig. 1), here we include this province in northwestern China. North China Plain (NCP), Beijing-Tianjin-Hebei (BTH), Yangtze River Delta (YRD), Pearl River Delta (PRD), and Sichuan Basin are also shown in the map. To evaluate and verify the spatial SO_2 VCD from OMI, we collected ground SO_2 monitoring data of 2014 through 2015 at 188 sampling sites (cities) across China (**Figure 1**), operated by the National Environmental Monitoring Center, available at http://www.aqistudy.cn/historydata. The statistics between OMI retrieved SO_2 VCD and monitored monthly and annually averaged SO_2 air concentrations during 2014-2015 at 188 operational air quality monitoring stations across China are presented in **Table S1** of Supplement. **Figure S1** is the correlation diagram between SO_2 VCD and sampled data. As shown in **Table S1** and **Fig. S1**, the OMI measured SO_2 VCDs agree well with the monitored ambient SO_2 concentrations across China at the correlation coefficient of 0.85 ($p<0.05$) (**Table S1**). **Figure 2** further compared annually averaged SO_2 VCDs and SO_2 air concentrations from 2005 to 2015 in 6 capital cities in Urumqi (Xinjiang), Yinchuan (Ningxia), Beijing (BTH and NCP), Shanghai (YRD), Guangzhou (PRD), and Chongqing (Sichuan Basin), respectively. The mean SO_2 concentration data were collected from provincial environmental bulletin published by the Ministry of Environmental Protection of China (MEPC) (http://www.zhb.gov.cn/hjzl/zghjzkgb/gshjzkgb. Results show that the annual variation of mean SO_2 VCDs match well with the monitored data except for Urumqi, the capital of Xinjiang Uygur Autonomous region. The OMI retrieved SO_2 VCDs in Shanghai and Chongqing are higher than the measured SO_2 concentrations from 2010 to 2015 but the both show consistent temporal fluctuation and trend. The measured SO_2 concentrations peaked in 2013 in Yinchuan whereas the SO_2 VCD reached the peak in 2012 and decreased thereafter. OMI measured SO_2 VCDs in Urumqi show different yearly fluctuations compared with its annual concentrations. The measured SO_2 concentrations in Urumqi decreased from 2011 to 2015 whereas the OMI measured SO_2 VCDs did not illustrate obvious changes. It is not clear the

Atmos. Chem. Phys. Discuss., doi:10.5194/acp-2017-161, 2017
Manuscript under review for journal Atmos. Chem. Phys.
Discussion started: 29 March 2017

causes leading to such the inconsistence. Measured concentrations might be subject to errors or not properly reported. Since the monitored SO_2 concentrations were collected in the urban area spatially averaged over 8 monitoring sites across the city whereas the OMI measured SO_2 VCD was averaged over all model grid points (0.25×0.25 latitude/longitude resolution) in Urumqi city. This could also result in the inconsistence between SO_2 VCD and measured data. However, such the error appeared not occurring in other cities.

SO_2 anthropogenic emission inventory in China with a 0.25° longitude by 0.25° latitude resolution for every two years from 2008 to 2012 was adopted from Multi resolution Emission Inventory for China (MEIC) (Li et al., 2017, available at http://www.meicmodel.org). The comparison between annual OMI SO_2 VCD and SO_2 emissions in China is presented in **Fig. 3**. As shown, the annual variation in SO_2 VCDs also agrees reasonably well with SO_2 emission data except for Midong. The OMI measured SO_2 VCD in the PRD and Sichuan Basin decreased from 2008 to 2012 but SO_2 emission changed little. Compared with the other five marked regions, the satellite measured SO_2 VCD in Midong declined in 2010 and inclined in 2012. However, SO_2 emissions in Midong increased in 2012 at about factor of 11 and 8 higher than that in 2008 and 2010. It should be noted that the MEIC SO_2 emission inventory from the bottom-up approach might be subject to large uncertainties due to the lack of sufficient knowledge in human activities and emissions from different sources (Li et al., 2017; Zhao et al., 2011; Kurokawa et al., 2013). From this perspective, the satellite remote sensing provides a powerful tool in monitoring SO_2

emissions from large point sources and the verification of emission inventories (Fioletov et al., 2016; Wang et al., 2015).

The socioeconomic data were collected from the China Statistical Yearbooks and China Energy Statistical Yearbook, published by National Bureau of Statistics of China (NBSC) (http://www.stats.gov.cn/tjsj/ndsj/;http://tongji.cnki.net/kns55/Navi/HomePage.aspx?id=N2010080088&name=YCXME&floor=1), as well as China National Environmental Protection Plan in the Eleventh Five-Years (2006-2010) and Twelfth Five-Years (2011-2015) released by MEPC (http://www.zhb.gov.cn).

2.3 Trends and step change

The long-term trends of SO_2 VCD were estimated by linear regressions of the gridded annually SO_2 VCD against their time sequence of 2005 through 2015. The gridded slopes (trends) of the linear regressions denote the increasing (positive) or decreasing (negative) rates of SO_2 VCD (Wang et al., 2016; Huang et al., 2015; Zhang et al., 2015, 2016).

The Mann-Kendall (MK) test was also employed in the assessments of the temporal trend and step change point year of SO_2 VCD time series. The MK test is a nonparametric statistical test (Mann,1945; Kendall, 1975), which is useful for assessing the significance of trends in time series data (Waked et al., 2016; Fathian et al., 2016). The MK test is often used to detect a step change point in the long term trend of a time series dataset (Moraes et al, 1998; Li et al., 2016; Zhao et al., 2016). It is suitable for non-normally distributed data and censored data which are not influenced by abnormal values (Yue and Pilon, 2004; Sharma et al 2016; Yue and

Atmos. Chem. Phys. Discuss., doi:10.5194/acp-2017-161, 2017
Manuscript under review for journal Atmos. Chem. Phys.
Discussion started: 29 March 2017

Wang., 2004; Gao et al 2016; Zhao et al., 2015). Recently, MK-test has also been used in trend analysis for the time series of atmospheric chemicals, such as persistent organic pollutants, surface ozone (O_3), and non-methane hydrocarbon (Zhao et al., 2015; Assareh et al.,2016; Waked et al.,2016; Sicard et al., 2016). Here the MK test was used to identify the temporal variability and step change point of SO_2 VCD for 2005-2015 which may be associated with the implementation of the national strategy and regulation in energy industry development and emission control during this period of time. Under the null hypothesis (no trend), the test statistic was determined using the following formula:

$$S_k = \sum_{i=1}^{k} r_i \ (k= 2, 3, ...,n) \tag{1}$$

where S_k is a statistic of the MK test, and

$$r_i = \begin{cases} +1, (x_i > x_j) \\ 0, (x_i \le x_j) \end{cases} \qquad (j=1,2, ...,i\text{-}1) \tag{2}$$

where x_i is the variable in time series x_1, x_2, ..., x_i, r_i is the cumulative number for $x_i > x_j$. The test statistic is normally distributed with a mean and variance given by:

$$E(S_k) = k(k-1)/4 \tag{3}$$

$$Var(S_k) = \frac{k(k-1)(2k+5)}{72} \tag{4}$$

From these two equations one can derive a normalized S_i, defined by

$$UF_k = \frac{S_k - E(S_k)}{\sqrt{Var(S_k)}} \quad (k=1, 2, ...,n) \tag{5}$$

where UF_k is the forward sequence, the backward sequence UB_k is calculated using the same function but with the reverse data series such that UB_k=-UF_k.

In a two-sided trend test, a null hypothesis is accepted at the significance level if $|(UF_k)| \leq (UF_k)_{1-\alpha/2}$, where $(UF_k)_{1-\alpha/2}$ is the critical value of the standard normal distribution, with a probability of *a*. When the null hypothesis is rejected (i.e., when any of the points in UF_k exceeds the confidence interval ±1.96; P=0.05), an significant increasing or decreasing trend is determined. $UF_k > 0$ often indicates an increasing trend, and vice versa. The test statistic used in the present study enables us to discriminate the approximate time of trend and step change by locating the intersection of the UF_k and UB_k curves. The intersection occurring within the confidence interval (-1.96, 1.96) indicates the beginning of a step change point (Moraeset al., 1998; Zhang et al., 2011; Zhao et al., 2015).

3 Results and discussion

3.1. Spatiotemporal variation in OMI measured SO_2

Given higher population density and stronger industrial activities, eastern and southern China are traditionally industrialized and heavily contaminated regions by air pollutions and acid rains caused by SO_2 emissions. **Figure 4a** shows annually averaged OMI SO_2 VCD over China on a 0.25° × 0.25° latitude/longitude resolution averaged from 2005 to 2015. SO_2 VCD was higher considerably in eastern and central China, and Sichuan Basin than that in northwestern China. The highest SO_2 VCD was found in the NCP, including Beijing-Tianjin-Hebei (BTH), Shandong, and Henan province. The annually averaged SO_2 VCD between 2005-2015 in this region reached 1.36 DU. This result is in line with previous satellite remote sensing retrieved SO_2 emissions in eastern China (Krotkov et al 2016; Lu et al., 2010; Bauduin et al., 2016; Jiang et al 2012; Yan et al., 2014). However, in contrast to the spatial distribution of decadal mean SO_2 VCD (**Fig. 4a**), the slopes of the linear regression relationship between annual average OMI-retrieved SO_2 VCD and the time sequence from 2005 to 2015 over China show that the negative trends overwhelmed industrialized eastern and southern China, particularly in the NCP, Sichuan Basin, the YRD, and PRD, manifesting significant decline of SO_2 emissions in these regions. SO_2 VCD in the PRD exhibited the largest decline at a rate of 7% yr^{-1}, followed by the NCP (6.7% yr^{-1}), Sichuan Basin (6.3% yr^{-1}), and the YRD (6% yr^{-1}), respectively. Annual average SO_2 VCD in the PRD, NCP, Sichuan Basin, and YRD decreased by 52%, 50% , 48%, and 46% in 2015 compared to 2005 (**Fig. 5**), though the annual fluctuation of SO_2 VCD shows rebounds in 2007 and 2011 which are potentially associated with the economic resurgence stimulated by the central government of China (He et al., 2009; Diao et al., 2012). The reduction of SO_2 VCD after 2011 in these regions reflects virtually the response of SO_2 emissions to the regulations in the reduction of SO_2 release, the mandatory application of the flue-gas desulfurization (FGD) on coal-fired power plants and heavy industries, and the slowdown in the growth rate of the Chinese economy (CSC, 2011a; Wang et al., 2015, Chen et al., 2016).

As also shown in **Fig. 4b**, in contrast to widespread decline of SO_2 VCD, there are two "hot spots" featured by moderate increasing trends of SO_2 VCD, located in the China's Energy Golden Triangle (EGT, Shen et al., 2016, Ma and Xu, 2017) and

Urumqi-Midong regions in northwestern China. The annual growth rate of SO_2 VCD from 2005 to 2015 are 3.4% yr^{-1} in the EGT and 1.8% yr^{-1} in Urumqi-Midong, respectively (**Fig. 4b**). Further details are presented in **Table 1**. SO_2 VCDs in these two regions peaked in 2011 and 2013 which were 1.6 and 1.7 times of that in 2005 (**Fig. 5**). The raising SO_2 VCDs in the part of the EGT have been reported by Shen et al. (2016). The second hot spot is located in Midong industrial park, about 40 km away from Urumqi, the capital of the Xinjiang Uygur Autonomous Region. The both EGT and Midong industrial parks are featured by extensive coal mining, thermal power generation, coal chemical, and coal liquefaction industries. The reserve of coal, oil and natural gas in the EGT is approximately 1.05×10^{12} ton of standard coal equivalent, accounting for 24% of the national total energy reserve in China (CRGECR, 2015). It has been estimated that there are deposits of 20.86 billion tons of oil, 1.03 billion cubic meters of natural gas, and 2.19 trillion tons of coal in Xinjiang, accounting for 30%, 34% and 40% of the national total (Dou, 2009). Over the past decades, a large number of energy-related industries have been constructed in northwestern China, such as the EGT and Midong chemical industrial parks in order to enhance China's energy security in the 21st century and speed up local economy. Rapid development of energy and coal chemical industries in Ningxia Hui Autonomous region and Xinjiang of northwestern China alone resulted in the significant demands to coal mining and coal products. The coal consumption, thermal power generation, and the gross industrial output increased by 2.7, 3.5, and 6.6 times in Ningxia from 2005 to 2015, and by 2.7, 4.2 and 6.6 times in Xinjiang during the same period (NBSC, 2005, 2015). As a result, SO_2 emissions increased markedly in these regions, as shown by the increasing trends of SO_2 VCD in the EGT and Midong (**Fig. 4b**). **Figure 6** illustrates the fractions of OMI measured annual SO_2 VCD and SO_2 emissions averaged over the 6 provinces of northwestern China in the annual national total VCD (**Fig. 6a**) and emissions (**Fig. 6b**) from 2005 to 2015. The both SO_2 VCD and emission fractions in northwestern China in the national total increased over the past decade. By 2015, the mean SO_2 VCD fraction in 6 northwestern provinces has reached 38% in the national total. The mean emission fraction was about 20% in the national total. It should be noted that there were large uncertainties in provincial SO_2 emission data which often underestimated SO_2 emissions from major point sources (Li et al., 2017; Han et al., 2007). In this sense, OMI retrieved SO_2 VCD fraction provides a more reliable estimate to the contribution of SO_2 emission in northwestern China to the national total.

The annual percentage changes in SO_2 VCD from 2005 onward are consistent well with per capita SO_2 emissions in China (**Fig. 7**). As aforementioned, while the annual total SO_2 emissions in the well developed BTH, YRD, and PRD were higher than that in northwestern provinces, the per capita emissions in all provinces of northwestern China, especially in Ningxia and Xinjiang, were about factors of 1 to 6 higher than that in the BTH, YRD, and PRD, as shown in **Fig. 7**. In contrast to declining annual emissions from the BTH, YRD, and PRD, the per capita SO_2 emissions in almost all western provinces have been growing from 2005 onward.

3.2 Trend and step changes in OMI measured SO_2 by MK test

Given that in the MK test the signs and fluctuations of UF_k are often used to predict the trend of a time series, this approach is further applied to quantify the trends and step changes in annually SO_2 VCD time series in those highlighted regions (a-f) in **Fig. 4b** from 2005 to 2015. Results are illustrated in **Fig. 8**. As shown, the forward and backward sequences UF_k and UB_k intersect at least once from 2005 to 2015. These intersections are all well within the confidence levels between -1.96 and 1.96 at the statistical significance α=0.01. A common feature of the forward sequence UF_k in eastern and southern China provinces is that UF_k has been declining and become negative from 2007 to 2009 onward **(Fig. 8a-d)**, confirming the downturn of SO_2 atmospheric emissions and levels in these industrialized and well developed regions in China. In the EGT and Midong areas of northwestern China (**Fig. 4b**), however, the UF_k values for SO_2 VCD are positive and growing, illustrating clear upward trends of SO_2 VCD over these two large-scale energy industry parks, revealing the response of SO_2 emissions to the energy industry relocation and development in northwestern China. To guarantee the national energy security and to promote the regional economy, the EGT energy program has been accelerating since 2003 under the national energy development and relocation plan (Zhu and Ruth, 2015; Chen et al., 2016), characterized by the rapid expansion of the Ningdong energy and chemical industrial base (NECIB) which is located about 40 km away from Yinchuan, the capital of Ningxia (Shen et al., 2016). By the end of 2010, a large number of coal chemical industries, including the world largest coal liquefaction and thermal power plants, have been built and operated, and the total installed capacity of thermal power

Atmos. Chem. Phys. Discuss., doi:10.5194/acp-2017-161, 2017
Manuscript under review for journal Atmos. Chem. Phys.
Discussion started: 29 March 2017

Atmospheric Chemistry and Physics Discussions
Open Access

generating units has reached 1.47 million kilowatts (Zhao, 2016). Under the same national plan, the Midong industrial park in Xinjiang started to construction and operation from the early to mid-2000s which has almost the same industrial structures as those in the EGT, featured by coal-fired power generation, coal chemical industry, and coal liquefaction.

For those regions with declining trends of SO_2 VCD, their step change points in the NCP, YRD and Sichuan Basin occurred between 2012 and 2013. These step change points coincide with the implementation of the new Ambient Air Quality Standard in 2012, which set a lower ambient SO_2 concentration limit in the air (MEPC, 2012), and the Air Pollution Prevention and Control Action Plan in 2013 by the State Council of China (CSC, 2013a). This Action Plan requests to take immediate actions to control and reduce air pollution in China, including cutting down industrial and mobile emission sources, adjusting industrial and energy structures, and promoting the application of clean energy in the BTH, YRD, PRD and Sichuan Basin. The step change in SO_2 VCD over the PRD occurred in the earlier year of 2009-2010 and from this period onward the decline of SO_2 VCD speeded up, as shown by the forward sequence UF_k which became negative since 2007 and was below the confidence level of -1.96 after 2009, suggesting significant decreasing VCD from 2009 (**Fig. 8c)**. In April 2002, the Hong Kong Special Administrative Region (HKSAR) Government and the Guangdong Provincial Government reached a consensus to reduce, on a best endeavor basis, the anthropogenic emissions of SO_2 by 40% in the PRD by 2010, using 1997 as the base year (http://www.epd.gov.hk/epd/english/action_blue_sky/files/exsummary_e.pdf). By the end of 2010, all thermal power units producing more than 0.125 million kilowatts electricity in the PRD were equipped with the FGD. During the 11th Five-Year Plan (2006-2010), the thermal power units with 1.2 million kilowatts capacity have been shut down. SO_2 emission was reduced by 18% in 2010 compared to that in 2005 (NBSC, 2006, 2011). This likely caused the occurrence of the step change in SO_2 VCD over 2009-2010.

The statistical significant step change points of SO_2 VCD in the EGT and Midong took place in 2006 and 2009, differing from those regions with decreasing trends of SO_2 VCD in eastern and southern China. The first step change point in 2006-2007 corresponds to the increasing SO_2 emissions in these two large-scale energy bases till their respective peak emissions in EGT (2007) and Midong (2008). The second step change point in 2009 coincides with the global financial crisis in 2008 which slowed down considerably the economic growth in 2009 in China, leading to raw material surplus and the remarkable reduction in the demand to coal products.

3.3 OMI SO_2 time series and step change point year in northwestern China

Since almost all large-scale coal chemical, thermal power generation, and coal liquefaction industries were built in energy-abundant and sparsely populated northwestern China over the past two decades, particularly since the early 2000s, those large-scale industrial parks and bases in this part of China likely play an important role in the growing SO_2 emissions in northwestern provinces. We further examine the OMI retrieved SO_2 VCD to confirm and evaluate the changes in SO_2 emissions in northwestern China which should otherwise respond to these large-scale energy programs under the national plan for energy relocation and expansion. **Figure 9** displays the MK test statistics for SO_2 VCD in the 6 provinces in northwestern China from 2005-2015. The forward sequence UF_k suggests decreasing trends in Shaanxi and Gansu provinces and a moderate increase in Qinghai province. In Xinjiang and Ningxia where the most energy industries were relocated and developed for the last decade (2005-2015), as aforementioned, UF_k time series estimated using SO_2 VCD data illustrate clear upward trends. Compared with those well developed regions in eastern and southern China, the UF_k values of SO_2 VCD in these northwestern provinces are almost all positive, except for Shaanxi province where the UF_k turned to negative from 2008， and Gansu province where the UF_k value become negative during 2012-2013.

The step change points identified by the MK test for SO_2 VCD in northwestern China appear associated strongly with the development and use of coal energy. As shown in **Fig. 9**, the intersection of the forward and backward sequences UF_k and UB_k within the confidence levels of -1.96 (straight green line) to 1.96 (straight purple line) can be identified in 2006 and 2007 in Ningxia and Xinjiang, respectively, corresponding well to the expansion of two largest energy industry bases from 2003 onward in Ningxia (NECIB) and Midong energy industry park in Xinjiang. The step change point of SO_2 VCD in 2012 in Gansu province coincides with fuel-switching from coal to gas in the capital city (Lanzhou) and many other places of the province initiated from 2012 (CSC, 2013b). The MK derived step change point in Shaanxi province occurs in 2010 which is a clear signal of marked decline of fossil fuel products in northern Shaanxi where, as the part of the EGT (Ma and Xu, 2017) of China, the largest energy industry base in the province is located, right after the global financial crisis.

It is interesting to note that the forward sequences UF_k of SO_2 VCD (**Fig. 9e** and **f)** in Ningxia and Xinjiang exhibit the similar fluctuations as that in Ningdong (NECIB) and Midong energy industrial bases (**Fig. 8e** and **f**), manifesting the potential associations between the SO_2 emissions in these two large-scale energy industrial parks (major point sources) and provincial emissions in Ningxia and Xinjiang, respectively. This suggests that large-scale energy industrial parks and bases might likely overwhelm or play an important role in the SO_2 emissions in those energy-abundant provinces in northwestern China. To assess the connections between the major point sources in the two energy industrial parks and the provincial emissions, we made use of OMI measured SO_2 VCD to inversely simulate the SO_2 emission burdens in Xinjiang and Ningxia. We used the source detection algorithm (McLinden et al., 2016) and the approach, which fits OMI-measured SO_2 vertical column densities to a three-dimensional parameterization function of the horizontal coordinates and wind speed, proposed by Fioletov et al. (2015, 2016), to estimate the SO_2 source strength in the two industrial parks and its contribution to the provincial total SO_2 burdens. **Figure 10** illustrates mean SO_2 burdens from 2005 to 2015 in northern Xinjiang (**Fig. 10a**) and Ningxia (**Fig. 10b**). The largest burdens can be seen clearly in the Midong energy industrial base and the NECIB in these two minority autonomous regions of China. Lower SO_2 emission burdens are illustrated in mountainous areas of northern Xinjiang. **Figure 11** illustrates the annual variations of estimated SO_2 emission burdens (10^{26} molecules) in the NECIB and Midong energy industrial parks (scaled on the left Y axis) and their respective fractions (%, scaled on the right Y axis) in the total provincial SO_2 burdens in Ningxia and Xinjiang, respectively. The SO_2 burden increased from 2005 and reached the maximum in 2011 in the NECIB and declined thereafter, in line with the annual SO_2 VCD fluctuations (**Fig. 5**) in this industrial park which is, as aforementioned, attributable to the economic rebound in 2011 in China. Of particular interest is the large fraction of the estimated SO_2 emission burden in the NECIB in Ningxia (**Fig. 11a**), showing that this industrial park alone contributed to about 40-50% emission burdens to the provincial total SO_2 emission burden. Likewise, the SO_2 emission burden enhanced from 2005 and peaked in 2013 in Midong energy industrial park (**Fig. 11b**). The emission burden in this park contributed about 25-35% to the provincial total SO_2 emission burden. Compared with the NECIB, the SO_2 emission burden is higher in the Midong industrial park but has the lower fraction in the provincial total emission burden. Covered by large area of desert and Gobi (Junngar Basin) underlying surfaces, there are only a few of SO_2 emission sources in vast northern Xinjiang region (total area of Xinjiang is 1.66×10^6 km^2), leading to the small ratio of the major point source (Midong) to total emission sources in Xinjiang. Nevertheless, overall our results manifest that, although there were only a small number of SO_2 point sources in these two energy industrial parks, the SO_2 emissions from these parks made significant contributions to provincial total emissions. Given that the national strategy for China's energy expansion and safety during the 21st century is, to a large extent, to develop large scale energy industrial parks in northwestern China, particularly in Xinjiang and Ningxia (Zhu and Ruth, 2015; Chen et al., 2016) where the energy resources are most abundant in China, we would expect that the rising SO_2 emissions in northwestern China would increasingly be attributed to those large scale energy industrial parks and contributed increasingly to the national total SO_2 emission in China.

Table 1 presents the annual average growth rates of SO_2 VCD, industrial (second) Gross Domestic Product (GDP), and major coal-consuming industries in northwestern China and three developed areas (BTH, YRD, PRD) in eastern and southern China. The positive growth rates of SO_2 VCD can be observed in the three province and autonomous regions (Qinghai, Ningxia, and Xinjiang) of northwestern China. Although the growth rates of SO_2 VCD in other two provinces (Gansu and Shaanxi) are negative, the magnitudes of the negative growth rates are smaller than those in the BTH, YRD, and PRD, except for Zhejiang province in the YRD. This regional contrast reflects both their economic and energy development activities, and the SO_2 emission control measures implemented by the local and central governments of China. Although China has set a national target of 10% SO_2 emission reduction (relative to 2005) during 2006-2010 and 8% (relative to 2010) during 2011-2015 (CSC, 2007; CSC, 2011b), under the Grand Western Development Program of China，the regulation for SO_2 emission control was waived in those energy-abundant provinces of northwestern China in order to speed up the large scale energy industrial bases and local economic development, and improve local personal income. In addition, although FGDs were widely installed in coal-fired power plants and other industrial sectors since the 1990s, by 2010 as much as 57% of these systems were installed in eastern and southern China (Zhao et al., 2013). The capacity of small power generators which were shut-down in western China was merely about 10808 MW, only accounting for about 19% of the capacity of total small power plants which were eliminated in China (55630 MW) during the 11th Five-Year Plan period (2006-2010) (Cui et al., 2016). As shown in **Table 1**, the SO_2 emission reduction plans virtually specified the zero percentage of SO_2 emission reductions in Qinghai, Gansu, and Xinjiang and lower reduction percentage in the emission reduction in Ningxia and Inner Mongolia as compared to eastern and southern China during the 11th (2006-2010) and 12th (2011-2015) Five-Year Plan. As a result, the average growth rate for thermal power generation, steel production, and coal consumption from 2005 to 2015 in northwestern China reached 14.1% yr^{-1}, 35.7% yr^{-1}, and 11.9% yr^{-1}, considerably higher than the averaged growth rates over eastern and southern China (5.9% yr^{-1} in the BTH,, 0.8% yr^{-1} in the YRD, and 2.3% yr^{-1} in the PRD).

4 Conclusions

The spatiotemporal variation in SO_2 concentration during 2005-2015 over China was investigated by making use of the PBL SO_2 column concentrations measured by the Ozone Monitoring Instrument. The highest SO_2 VCD was found in the NCP, the most heavily polluted area by SO_2 and particular matters (PM) in China, including Beijing-Tianjin-Hebei, Shandong, and Henan province. Under the national regulation for SO_2 control and emission reduction, the SO_2 VCD in eastern and southern China underwent widespread decline during this period. However, the OMI measured SO_2 VCD detected two "hot spots" in the EGT (Ningxia-Shaanxi-Inner Mongolia) and Midong (Xinjiang) energy industrial parks, in contrast to the declining SO_2 emissions in eastern and southern China, displaying an increasing trend with the annual growth rate of 3.4% yr^{-1}in the EGT and 1.8% yr^{-1} in Midong, respectively. The trend analysis further revealed enhanced SO_2 emissions in most provinces of northwestern China likely due to national strategy for energy industry expansion and relocation in energy-abundant northwestern China. As a result, per capita SO_2 emission in northwestern China has exceeded industrialized and populated eastern and southern China, making increasing contributions to the national total SO_2 emission. The estimated SO_2 emission burdens in the Ningdong (Ningxia) and Midong (Xinjiang) energy industrial parks from OMI measured SO_2 VCD showed that the SO_2 emissions in these two industrial parks made significant contributions to the provincial total emissions. This indicates, on one side, that the growing SO_2 emissions in northwestern China would increasingly come from those large scale energy industrial parks under the national energy development and relocation plan. On the other side, this fact also suggests that it is likely more straightforward to control and reduce SO_2 emissions in northwestern China because the SO_2 control measures could be readily implemented and authorized in those state-owned large-scale energy industrial bases.

The Supplement related to this article is available online

Acknowledgements. This work is supported by the National Natural Science Foundation of China (grants 41503089, 41371478, and 41671460), Gansu Province Science and Technology Program for Livelihood of the People (1503FCMA003), the Natural Science Foundation of Gansu Province of China (1506RJZA212), and Fundamental Research Funds for the Central Universities (lzujbky-2016-249 and lzujbky-2016-253). We thank Dr. Vitali Fioletov for his suggestions and advices during the course of preparation of this manuscript.

Reference

Assareh, N., Prabamroong, T., Manomaiphiboon, K., Theramongkol, P., Leungsakul, S., Mitrjit, N., and Rachiwong, J.: Analysis of observed surface ozone in the dry season over Eastern Thailand during 1997–2012, Atmos. Res., 178, 17-30, doi: 10.1016/j.atmosres.2016.03.009, 2016.

Bauduin, S., Clarisse, L., Hadji-Lazaro, J., Theys, N., Clerbaux, C., and Coheur, P. F.: Retrieval of near-surface sulfur dioxide (SO_2) concentrations at a global scale using IASI satellite observations, Atmos. Meas. Tech., 9, 721-740, doi: 10.5194/amt-9-721-2016, 2016.

BIEE (British Institute of Energy Economics): BP Statistical Review of World

Atmos. Chem. Phys. Discuss., doi:10.5194/acp-2017-161, 2017
Manuscript under review for journal Atmos. Chem. Phys.
Discussion started: 29 March 2017

Energy June 2016, Available at: http://www.bp.com/content/dam/bp/pdf/energy-economics/statistical-review-2016/bp-statistical-review-of-world-energy-2016-full-report.pdf (last access: 21 January 2017), 2016.

Chen, J., Cheng, S.; Song, M., and Wang, J.: Interregional differences of coal carbon dioxide emissions in China, Energ. Policy, 96, 1−13, doi: 10.1016/j.enpol.2016.05.015, 2016.

CRGECR (The Comprehensive Research Group for Energy Consulting and Research): Strategy on the Development of Energy "Golden Triangle", Engineering Science., 9,18-28, 2015 (in Chinese).

CSC (China's State Council): China National Environmental Protection Plan in the 11th Five-year (2006-2010), Available at: http://www.gov.cn/zwgk/2007-11/26/content_815498.htm (last access: 21 January 2017), 2007 (in Chinese).

CSC (China's State Council): Circular on accelerating the number of comments on shutting down small thermal power units in China, Available at http://www.gov.cn/zwgk/2007-01/26/content_509911.htm (last access: 21 January 2017), 2011a (in Chinese).

CSC (China's State Council): China National Environmental Protection Plan in the 12th Five-year (2011-2015), Available at: http://www.gov.cn/zwgk/2011-12/20/content_2024895.htm (last access: 21 January 2017), 2011b (in Chinese).

CSC (China's State Council): Air Pollution Prevention and Control Action Plan, Available at: http://www.gov.cn/zhengce/content/2013-09/13/content_4561.htm (last access: 21 January 2017), 2013a (in Chinese).

CSC (China's State Council): Determination, Measures and Strength-Lanzhou pollution control reproduce the blue sky, Available at: http://www.gov.cn/jrzg/2013-02/03/content_2325835.htm (last access: 21 January 2017), 2013b (in Chinese).

Cui, Y., Lin, J., Song, C., Liu, M., Yan, Y., Xu, Y., and Huang, B.: Rapid growth in nitrogen dioxide pollution over Western China, 2005-2013. Atmos. Chem. Phys., 16, 6207-6221, doi: 10.5194/acp-16-6207-2016, 2016.

Diao, X., Zhang, Y., and Chen, K. Z.: The global recession and China's stimulus package: A general equilibrium assessment of country level impacts, China. Econ. Rev., 23, 1-17, doi: 10.1016/j.chieco.2011.05.005, 2012.

Dou, L.: A research on the impact of industrialization on the environment in Xinjiang with an empirical analysis, Mater thesis, Xinjiang University, Urumqi, 2009 (in Chinese).

Fathian, F., Dehghan, Z., Bazrkar, M. H., and Eslamian, S.: Trends in hydrological and climatic variables affected by four variations of the Mann-Kendall approach in Urmia Lake Basin, Iran. Hydrolog. Sci. J., 61, 892-904, doi: 10.1080/02626667.2014.932911, 2016.

Fioletov, V. E., McLinden, C. A.,Krotkov, N., and Li, C.: Lifetimes and emissions of SO_2 from point sources estimated from OMI, Geophys. Res. Lett., 42, 1969-1976, doi: 10.1002/2015GL063148, 2015.

Fioletov, V. E., McLinden, C. A., Krotkov, N., Li, C., Joiner, J., Theys, N., Carn, S., and Moran, M. D.: A global catalogue of large SO_2 sources and emissions derived from the Ozone Monitoring Instrument, Atmos. Chem. Phys., 16, 11497–11519, doi: 10.5194/acp-16-11497-2016, 2016.

Gao, T., and Shi, X.: Spatio-temporal characteristics of extreme precipitation events during 1951-2011 in Shandong, China and possible connection to the large scale atmospheric circulation, Stoch. Env. Res. Risk. A., 30, 1421-1440, doi: 10.1007/s00477-015-1149-7, 2016.

Han, Y.; Gao, J.; Li, H; and Li, Y.: Ecological suitability analysis on the industry overall arrangement plan of Ningdong energy sources and chemical industry base, Environ. Sci. Manager, 32, 142-147,2007 (in Chinese).

He, D., Zhang, Z., and Zhang, W.: How large will be the effect of China's fiscal stimulus package on output and employment, Pacific Economic Review, 14, 730-744, doi: 10.1111/j.1468-0106.2009.00480.x, 2009.

Huang, T., Jiang, W., Ling, Z., Zhao, Y., Gao, H., and Ma, J.: Trend of cancer risk of Chinese inhabitants to dioxins due to changes in dietary patterns 1980-2009, Sci. Rep., 6, doi: 10.1038/srep21997, 2016.

Ialongo, I., Hakkarainen, J., Kivi, R., Anttila, P., Krotkov, N. A.,Yang, K., Li, C., Tukiainen, S., Hassinen, S., and Tamminen, J.: Comparison of operational satellite SO_2 products with ground-based observations in northern Finland during the Icelandic Holuhraun fissure eruption, Atmos. Meas. Tech., 8, 2279-2289, doi:

10.5194/amt-8-2279-2015, 2015.

Jiang, J., Zha, Y., Gao, J., and Jiang, J.: Monitoring of SO_2 column concentration change over China from Aura OMI data, Int. J. Remote Sen., 33, 1934-1942, doi: 10.1080/01431161.2011.603380, 2012.

Kanada, M., Dong, L., Fujita, T., Fujita, M., Inoue, T., Hirano, Y., Togawa, T., and Geng, Y.: Regional disparity and cost-effective SO_2 pollution control in China: A case study in 5 mega-cities, Energ. Policy, 61, 1322-1331, doi:10.1016/j.enpol.2013.05.105, 2013.

Kendall, M. G., and Charles, G.: Rank correlation methods, Oxford Univ. Press, New York., USA, 202 pp., 1975.

Krotkov, N. A., McLinden, C. A., Li, C., Lamsal, L. N., Celarier, E. A., Marchenko, S. V., Swartz, W. H., Bucsela, E. J., Joiner, J., Duncan, B. N., Boersma, K. F., Veefkind, J. P., Levelt, P. F., Fioletov, V. E., Dickerson, R. R., He, H., Lu, Z., and Streets, D. G.: Aura OMI observations of regional SO_2 and NO_2 pollution changes from 2005 to 2015, Atmos. Chem. Phys., 16, 4605-4629, doi: 10.5194/acp-16-4605-2016, 2016.

Kurokawa, J., Ohara, T., Morikawa, T., Hanayama, S., Greet, J. M., G., Fukui, T., Kawashima, K., and Akimoto, H.: Emissions of air pollutants and greenhouse gases over Asian regions during 2000–2008: Regional Emission inventory in Asia (REAS) version 2, Atmos. Chem. Phys., 13, 11019–11058, doi: 10.5194/acp-13-11019-2013, 2013.

Li, C., Joiner, J., Krotkov, N. A., and Bhartia, P. K.: A fast and sensitive new satellite

SO_2 retrieval algorithm based on principal component analysis: Application to the Ozone Monitoring Instrument, Geophys. Res. Lett., 40, 6314-6318, doi: 10.1002/2013GL058134,2013.

Li, C., Wang, R., Ning, H., and Luo, Q.: Changes in climate extremes and their impact on wheat yield in Tianshan Mountains region, northwest China, Environ. Earth Sci., 75, doi: 10.1007/s12665-016-6030-6, 2016.

Li, C., Zhang, Q., Krotkov, N. A., Streets, D. G., He, K., Tsay, S. C., and Gleason, J. F.: Recent large reduction in sulfur dioxide emissions from Chinese power plants observed by the Ozone Monitoring Instrument, Geophys. Res. Lett., 37, L08807, doi: 10.1029/2010GL042594, 2010.

Li, M., Zhang, Q., Kurokawa, J., Woo, J., He, K., Lu, Z., Ohara, T., Song, Y., Streets, D. G., Carmichael, G. R., Cheng, Y., Hong, C., Huo, H., Jiang, X., Kang, S., Liu, F., Su, H., and Zheng, B.: MIX: a mosaic Asian anthropogenic emission inventory under the international collaboration framework of the MICS-Asia and HTAP, Atmos. Chem. Phys., 17, 935-963, doi: 10.5194/acp-17-935-2017, 2017.

Lu, Z., Streets, D. G., Zhang, Q., Wang, S., Carmichael, G. R.,Cheng, Y. F., Wei, C., Chin, M., Diehl, T., and Tan, Q.: Sulfur dioxide emissions in China and sulfur trends in East Asia since 2000, Atmos. Chem. Phys., 10, 6311-6331, doi: 10.5194/acp-10-6311-2010, 2010.

Lu, Z., Zhang, Q., and Streets, D. G.: Sulfur dioxide and primary carbonaceous aerosol emissions in China and India, 1996-2010, Atmos. Chem. Phys., 11, 9839-9864,doi: 10.5194/acp-11-9839-2011, 2011.

Ma, J., and Xu, J.: China's energy rush harming ecosystem, Nature, 541-30, doi: 10.1038/541030b, 2017.

Mann, H. B.: Nonparametric tests against trend, Econometrica, 13, 245-259, doi: 10.2307/1907187, 1945.

McLinden, C. A., Fioletov, V., Krotkov, N. A., Li, C., Boersma, K. F., and Adams, C.: A decade of change in NO_2 and SO_2 over the Canadian oil sands as seen from space, Environ. Sci. Technol., 50, 331-337, doi: 10.1021/acs.est.5b04985, 2015.

McLinden, C. A., Fioletov, V., Shephard, M. W., Krotkov, N., Li, C., Martin, R. V., Moran, M. D., and Joiner, J.: Space-based detection of missing sulfur dioxide sources of global air pollution, Nature Geosci., 9, 496-500, doi: 10.1038/ngeo2724, 2016.

MEPC (Ministry of Environmental Protection of China): Ambient air quality standards, Available at: http://kjs.mep.gov.cn/hjbhbz/bzwb/dqhjbh/dqhjzlbz/201203/t20120302_224165.shtml (last access:21 January 2017), 2012 (in Chinese).

Moraes, J. M., Pellegrino, G. Q., Ballester, M. V., Martinelli, L. A., Victoria, R. L., and Krusche, A. V.: Trends in hydrological parameters of a southern Brazilian watershed and its relation to human induced changes, Water Resour. Manag., 12, 295-311, doi: 10.1023/A:1008048212420, 1998.

NBSC(National Bureau of Statistics of China): China Energy Statistical Yearbook 2005,China Statistics Press, Beijing, 2005.

NBSC(National Bureau of Statistics of China): China Energy Statistical Yearbook

2006, China Statistics Press, Beijing, 2006.

NBSC(National Bureau of Statistics of China): China Energy Statistical Yearbook 2011,China Statistics Press, Beijing, 2011.

NBSC(National Bureau of Statistics of China): China Energy Statistical Yearbook 2015,China Statistics Press, Beijing, 2015.

Ohara, T., Akimoto, H., Kurokawa, J., Horii, N., Yamaji, K., Yan, X., and Hayasaka, T.: An Asian emission inventory of anthropogenic emission sources for the period 1980–2020, Atmos. Chem. Phys., 7, 4419-4444, doi: 10.5194/acp-7-4419-2007, 2007.

Sharma, C. S., Panda, S. N., Pradhan, R. P., Singh, A., and Kawamura, A.: Precipitation and temperature changes in eastern India by multiple trend detection methods, Atmos. Res., 180, 211-225, doi: 10.1016/j.atmosres.2016.04.019, 2016.

Shen, Y., Zhang, X., Brook, J. R., Huang, T., Zhao, Y., Gao, H., and Ma, J.: Satellite remote sensing of air quality in the Energy Golden Triangle in Northwest China, Environ. Sci. Technol. Lett., 3,275-279, doi: 10.1021/acs.estlett.6b00182, 2016.

Sicard, P., Serra, R., and Rossello, P.: Spatiotemporal trends in ground-level ozone concentrations and metrics in France over the time period 1999-2012, Environ. Res., 149, 122-144, doi:10.1016/j.envres.2016.05.014, 2016.

Smith, S. J., van Aardenne, J., Klimont, Z., Andres, R. J.,Volke, A., and Delgado Arias, S.: Anthropogenic sulfur dioxide emissions: 1850-2005, Atmos. Chem. Phys., 11, 1101-1116,doi:10.5194/acp-11-1101-2011, 2011.

Stevenson, D. S., Johnson, C. E., Collins, W. J., and Derwent,R. G.: The atmospheric sulphur cycle and the role of volcanic SO_2, Geol. Soc. Lond. Spec. Publ., 213, 295-305, doi: 10.1144/GSL.SP.2003.213.01.18, 2003.

Su, S., Li, B., Cui, S., and Tao, S.: Sulfur Dioxide Emissions from Combustion in China: From 1990 to 2007, Environ. Sci. Technol., 45, 8403-8410, doi: 10.1021/es201656f, 2011.

Waked, A., Sauvage, S., Borbon, A., Gauduin, J., Pallares, C., Vagnot, M. P., Thierry, L., and Locoge, N.: Multi-year levels and trends of non-methane hydrocarbon concentrations observed in ambient air in France, Atmos. Environ., 141, 263-275, doi: 10.1016/j.atmosenv.2016.06.059, 2016.

Wang, S., Zhang, Q., Martin, R.V., Philip, S., Liu, F., Li, M., Jiang, X., and He, K.: Satellite measurements oversee China's sulfur dioxide emission reductions from coal-fired power plants, Environ. Res. Lett., 10, 114015, doi: 10.1088/1748-9326/10/11/114015, 2015.

Wang, S., Satellite remote sensing of the sulfur dioxide and nitrogen dioxide emissions from coal-fired power plants, PhD thesis, Tsinghua University, Beijing, 2014.

Wang, Z., Shao, M., Chen, L., Tao, M., Zhong, L., Chen, D., Fan, M., Wang, Y., and Wang, X.: Space view of the decadal variation for typical air pollutants in the Pearl River Delta (PRD) region in China, Front. Env. Sci. Eng., 10, doi: 10.1007/s11783-016-0853-y, 2016.

Whelpdale, D. M., Dorling, S. R., Hicks, B. B., and Summers, P.W.: Atmospheric process in: Global Acid Deposition Assessment, edited by: Whelpdale, D. M., and Kaiser, M. S., World Meteorological Organization Global Atmosphere Watch, Report Number 106, Geneva, 7-32, 1996.

Yan, H., Chen, L., Su, L., Tao, J., and Yu, C.: SO_2 columns over China: Temporal and spatial variations using OMI and GOME-2 observations, 35th International Symposium on Remote Sensing of Environment, 17, 012027, doi: 10.1088/1755-1315/17/1/012027, 2014.

Yue, S and Pilon, P.: A comparison of the power of the t test, Mann- Kendall and bootstrap tests for trend detection, Hydrolog. Sci. J., 49, 21-37, doi: 10.1623/hysj.49.1.21.53996, 2004.

Yue, S., and Wang, C.: The Mann-Kendall test modified by effective sample size to detect trend in serially correlated hydrological series, Water Resour. Manag., 18, 201-218, doi: 10.1023/B:WARM.0000043140.61082.60, 2004.

Zhang, X., Huang, T., Zhang, L., Gao, H., Shen, Y., and Ma, J.: Trends of deposition fluxes and loadings of sulfur dioxide and nitrogen oxides in the artificial Three Northern Regions Shelter Forest across northern China, Environ. Pollut., 207, doi: 10.1016/j.envpol.2015.09.022 238-247, 2015.

Zhang, X., Huang, T. Zhang, L., Shen, Y., Zhao, Y., Gao, H., Mao, X., Jia, C., and Ma, J.: Three-North Shelter Forest Program contribution to long-term increasing trends of biogenic isoprene emissions in northern China, Atmos. Chem. Phys., 16, 6949-6960, doi: 10.5194/acp-16-6949-2016, 2016.

Zhang, Y., Guan, D., Jin, C., Wang, A., Wu, J., and Yuan, F.: Analysis of impacts of climate variability and human activity on stream flow for a river basin in northeast China, J. Hydrol., 410, 239-247, doi: 10.1016/j.jhydrol.2011.09.023, 2011.

Zhao, B., Wang, S. X., Liu, H., Xu, J. Y., Fu, K., Klimont, Z., Hao,J. M., He, K. B., Cofala, J., and Amann, M.: NOx emissions in China: historical trends and future perspectives, Atmos. Chem. Phys., 13, 9869–9897, doi: 10.5194/acp-13-9869-2013, 2013.

Zhao, L.: Strategic thinking on construction of Ningdong Energy Chemical Base and development of Ningxia Coal Industry Group, Northwest Coal, 4, 11-13, 2016 (in Chinese).

Zhao, Y., Huang, T., Wang, L., Gao, H., and Ma, J.: Step changes in persistent organic pollutants over the Arctic and their implications, Atmos. Chem. Phys., 15, 3479-3495, doi: 10.5194/acp-15-3479-2015, 2015.

Zhao, Y., Nielsen, C. P., Lei, Y., McElroy, M. B., and Hao, J.: Quantifying the uncertainties of a bottom-up emission inventory of anthropogenic atmospheric pollutants in China, Atmos. Chem. Phys., 11, 2295–2308, doi: 10.5194/acp-11-2295-2011, 2011.

Zhu, J.; and Ruth, M.: Relocation or reallocation: Impacts of differentiated energy saving regulation on manufacturing industries in China, Ecol. Econ., 110, 119−133, doi: 10.1016/j.ecolecon.2014.12.020, 2015.

Atmos. Chem. Phys. Discuss., doi:10.5194/acp-2017-161, 2017
Manuscript under review for journal Atmos. Chem. Phys.
Discussion started: 29 March 2017

Atmospheric Chemistry and Physics Discussions
Open Access
EGU

Table 1 Annual growth rate for OMI SO_2 VCD and economic activities for individual provinces and municipality during 2005-2014 (%yr^{-1}), and SO_2 emission reduction plan during the 11th and 12th Five-Year Plan period (%).

Region		OMI SO_2 VCD	coal consumption	Industrial GDP	Thermal power generation	steel production	SO_2 emission reduction plan (%)	
							2006-2010[a]	2011-2015[b]
Northwestern	Inner Mongolia	0.94	11.29	20.48	14.07	8.38	-3.8	-3.8
	Shaanxi	-3.41	13.14	19.96	13.01	14.48	-12	-7.9
	Gansu	-0.09	6.69	14.19	8.89	9.92	0	2.0
	Qinghai	0.69	11.20	18.70	9.88	12.37	0	16.7
	Ningxia	0.95	11.79	17.44	15.04	152.71	-9.3	-3.6
	Xinjiang	1.57	17.21	14.21	23.39	16.27	0	0
BTH	Beijing	-3.59	-6.13	9.13	5.99	-48.52	-20.4	-13.4
	Tianjin	-4.63	3.15	15.84	6.01	10.19	-9.4	-9.4
	Hebei	-5.05	4.16	12.37	6.22	10.70	-15	-12.7
YRD	Shanghai	-7.65	-0.93	6.64	0.86	-0.92	-26.9	-13.7
	Jiangsu	-5.93	5.39	12.51	7.49	13.35	-18.0	-14.8
	Zhejiang	-2.07	4.04	11.40	8.68	13.94	-15.0	-13.3
PRD	Guangdong	-4.55	6.15	12.03	5.92	6.87	-15.0	-14.8

a and b represents proposed reduction in SO_2 emission in 2010 relative to 2005, and 2015 relative to 2010, respectively. The value for PRD refers to the proposed target for Guangdong Province.

Figure Captions

Figure 1 Provinces, autonomous regions, and selected regions in China in this investigation. Northwestern China, defined by pink slash, includes Inner Mongolia, Shaanxi, Gansu, Qinghai, Ningxia, and Xinjiang province. Light green shadings with cross highlight Beijing-Tianjin-Hebei (BTH) and the light green color stands for the North China Plain (NCP, including BTH), defined by light green color, including BTH, Shandong, and Henan province. The Sichuan Basin, Yangtze River Delta (YRD), and Pearl River Delta (PRD) is defined by yellow, pink, and blue color. Red triangle indicate 188 monitoring sites across China.

Figure 2 Annually averaged SO_2 VCD (DU), scaled on the right-hand-side Y-axis and measured annual SO_2 air concentration (μg/m^3), scaled on the left-hand-side Y-axis, in Beijing, Shanghai, Chongqing, Guangzhou, Yinchuan, and Urumqi.

Figure 3 Annually averaged SO2 VCD (DU), scaled on the right-hand-side Y-axis and annual emissions (thousand ton/yr) of SO2 on the left-hand-side Y-axis in the NCP, YRD, PRD, Sichuan Basin, EGT, and Midong.

Figure 4 Annual averaging OMI-retrieved vertical column densities of SO_2 (DU) and their trends from 2005 to 2015 on 0.25° × 0.25° latitude/longitude resolution in China. (**a**). Annual mean SO_2 vertical column densities; (**b**). slope (trend) of linear regression relationship between annual average OMI-retrieved SO_2 VCD and the time sequence from 2005 to 2015 over China. The positive values indicate an increasing trend of SO_2 VCD from 2005 to 2015, and vice versa. The blue circle highlights the six selected regions where SO_2 VCD displayed dramatic change for further assessment of the long term trends and step change points in SO_2 VCD. These six regions are NCP (a), YRD (b), PRD (c), Sichuan Basin (d), Energy Golden Triangle (EGT, e), and Midong (f).

Figure 5 Percentage changes in annual mean OMI SO_2 VCD in the four highlighted regions in eastern and southern China and two large-scale energy industry parks in the EGT and Midong region in **Figure 4b** (relative to 2005).

Figure 6 Annual fractions of OMI retrieved SO_2 VCD and emissions averaged over 6 northwestern provinces in the national total SO_2 VCD from 2005 to 2015 and emission from 2005 to 2014. (**a**) fraction of annual mean SO_2 VCD; (**b**) fraction of annual mean emission. Fractions of SO_2 VCD are calculated as the ratio of the sum of annually averaged SO_2 VCD in northwestern China to the sum of annually averaged SO_2 VCD in the national total from 2005 to 2015 (%).

Figure 7 Per capita SO_2 emission in six provinces of northwestern China and three key eastern regions (tons/person). The value for PRD refers to the per capita SO_2 emission for Guangdong province.

Figure 8 Mann-Kendall (MK) test statistics for annually SO_2 VCD in those highlighted regions (**Figs. 1** and **4b)** from 2005-2015. The blue solid line is the forward sequence UF_k and the red solid line is the backward sequence UB_k defined by Eq (5). The positive values for UF_k indicate an increasing trend of SO_2 VCD, and vice versa. Two straight solid lines stand for confidence interval between -1.96 (straight green line) and 1.96 (straight purple line) in the MK test. The bold black line in the middle highlights zero value of UF_k and UB_k. The bold black line in the

Atmos. Chem. Phys. Discuss., doi:10.5194/acp-2017-161, 2017
Manuscript under review for journal Atmos. Chem. Phys.
Discussion started: 29 March 2017

middle highlights zero value of UF_k and UB_k. The intersection of UF_k and UB_k sequences within the intervals between two confidence levels indicates a step change point.

Figure 9 Mann-Kendall (MK) test statistics for annually SO_2 VCD in six provinces in northwestern China from 2005-2015. The blue solid line is the forward sequence UF_k and the red solid line is the backward sequence UB_k defined by Eq (5). The positive values for UF_k indicate an increasing trend of SO_2 VCD, and vice versa. Two straight solid lines stand for confidence interval between -1.96 (straight green line) and 1.96 (straight purple line) in the MK test. The intersection of UF_k and UB_k sequences within intervals between two confidence levels indicates a step change point.

Figure 10 Mean SO_2 burden estimated by the OMI measured SO_2 VCD (DU) using a new emission detection algorithm (Fioletov et al., 2016). (**a**) SO_2 burden in northern Xinjiang; (**b**) SO_2 burden in Ningxia.

Figure 11 Annual SO_2 burdens (10^{26} molecule) in the Ningdong and Midong energy industrial parks and their fractions in provincial total SO_2 burden. (**a**). SO_2 burden (blue bar) in Ningdong and its fraction (red solid line) in the total provincial SO_2 burden in Ningxia; (**b**). SO_2 burden (blue bar) in Midong and its fraction (red solid line) in the total provincial SO_2 burden in Xinjiang. The left Y-axis stands for SO_2 emission burden and the right Y-axis denotes the fraction (%).

Atmos. Chem. Phys. Discuss., doi:10.5194/acp-2017-161, 2017
Manuscript under review for journal Atmos. Chem. Phys.
Discussion started: 29 March 2017

Atmospheric Chemistry and Physics
Open Access
Discussions

Figure 1

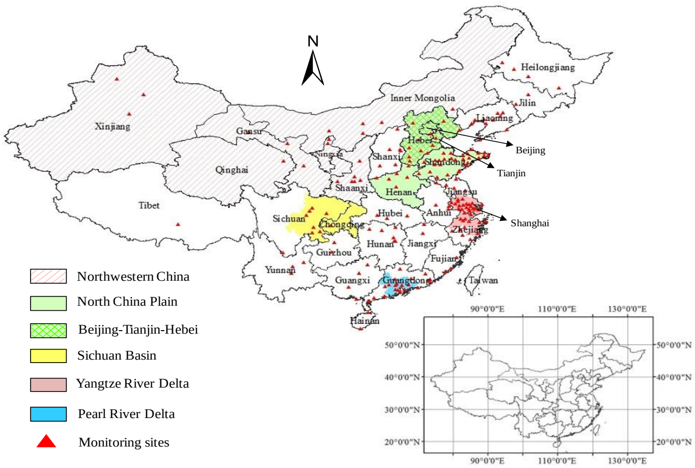

Atmos. Chem. Phys. Discuss., doi:10.5194/acp-2017-161, 2017
Manuscript under review for journal Atmos. Chem. Phys.
Discussion started: 29 March 2017

Figure 2

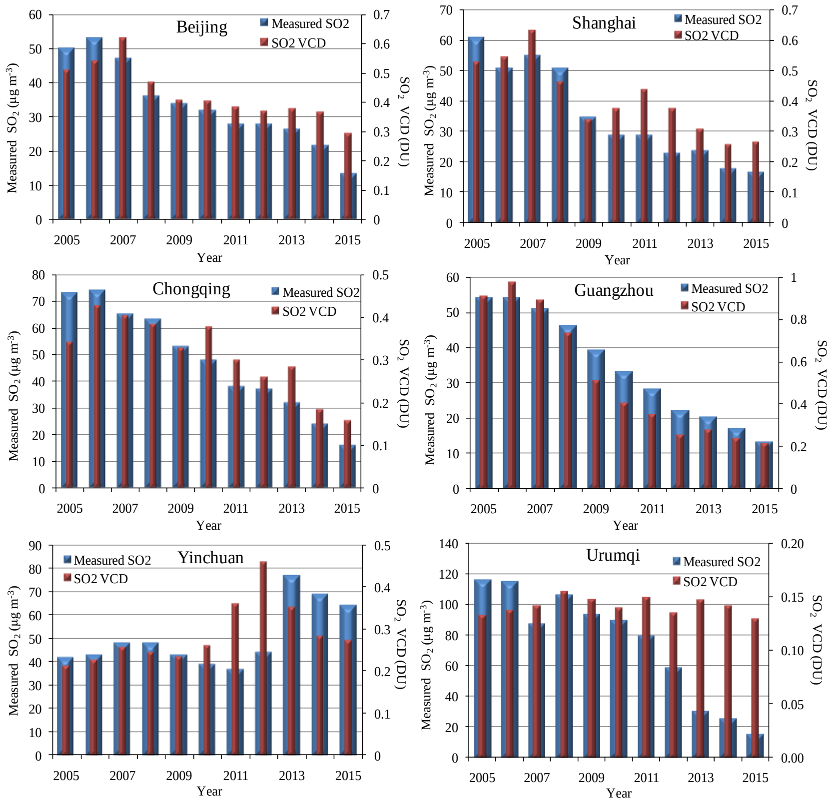

Atmos. Chem. Phys. Discuss., doi:10.5194/acp-2017-161, 2017
Manuscript under review for journal Atmos. Chem. Phys.
Discussion started: 29 March 2017

Atmospheric Chemistry and Physics Discussions

Figure 3

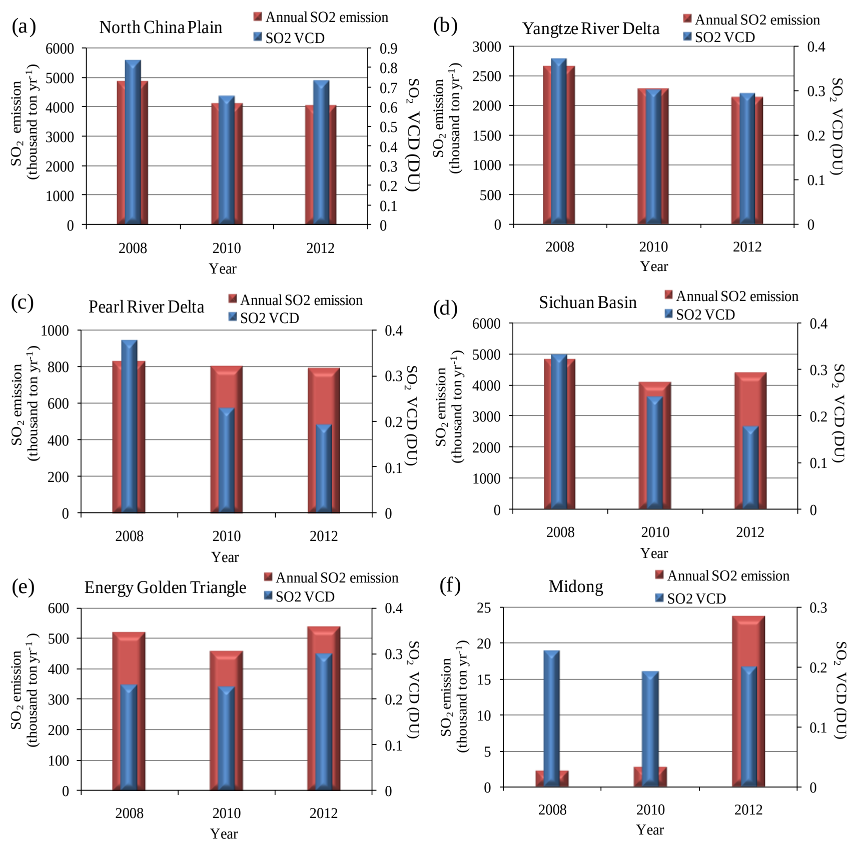

Atmos. Chem. Phys. Discuss., doi:10.5194/acp-2017-161, 2017
Manuscript under review for journal Atmos. Chem. Phys.
Discussion started: 29 March 2017

Figure 4

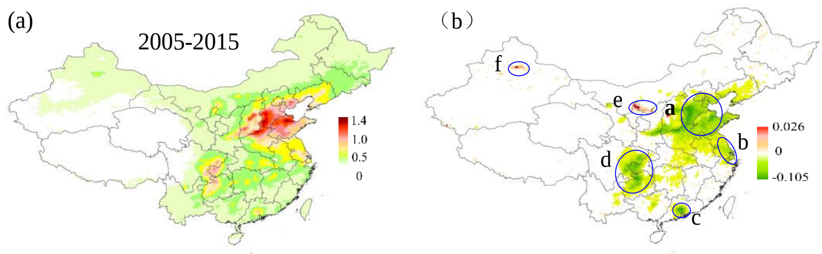

Figure 5

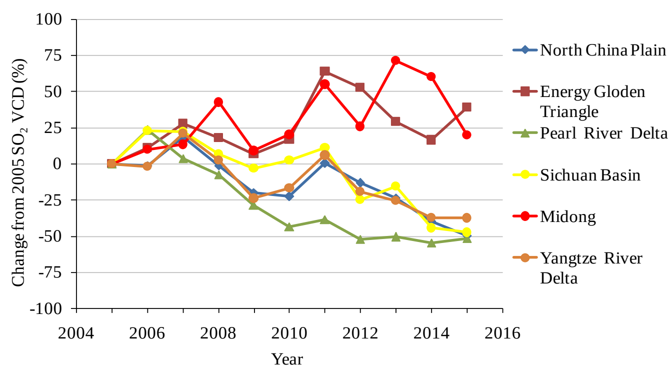

Atmos. Chem. Phys. Discuss., doi:10.5194/acp-2017-161, 2017
Manuscript under review for journal Atmos. Chem. Phys.
Discussion started: 29 March 2017

Atmospheric Chemistry and Physics
Discussions
Open Access

Figure 6

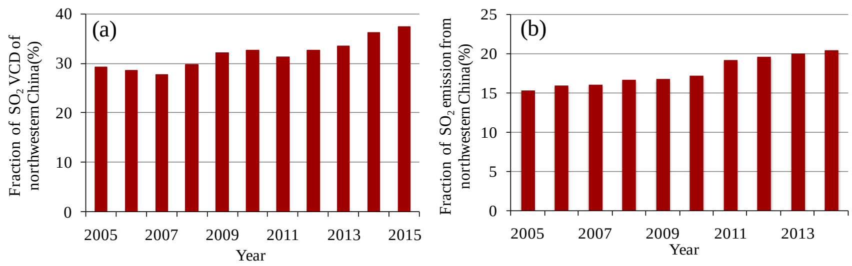

Figure 7

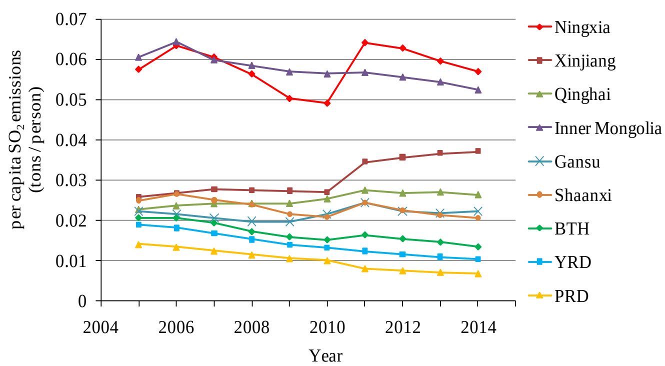

Atmos. Chem. Phys. Discuss., doi:10.5194/acp-2017-161, 2017
Manuscript under review for journal Atmos. Chem. Phys.
Discussion started: 29 March 2017

Atmospheric Chemistry and Physics
Open Access
EGU
Discussions

Figure 8

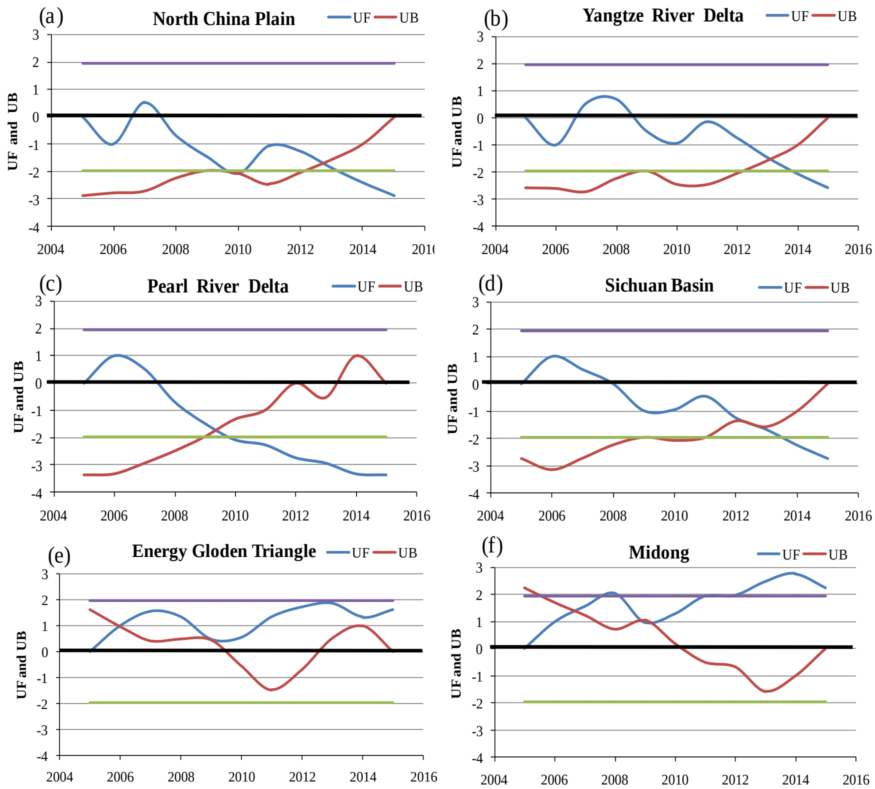

Atmos. Chem. Phys. Discuss., doi:10.5194/acp-2017-161, 2017
Manuscript under review for journal Atmos. Chem. Phys.
Discussion started: 29 March 2017

Atmospheric Chemistry and Physics
Open Access
Discussions

Figure 9

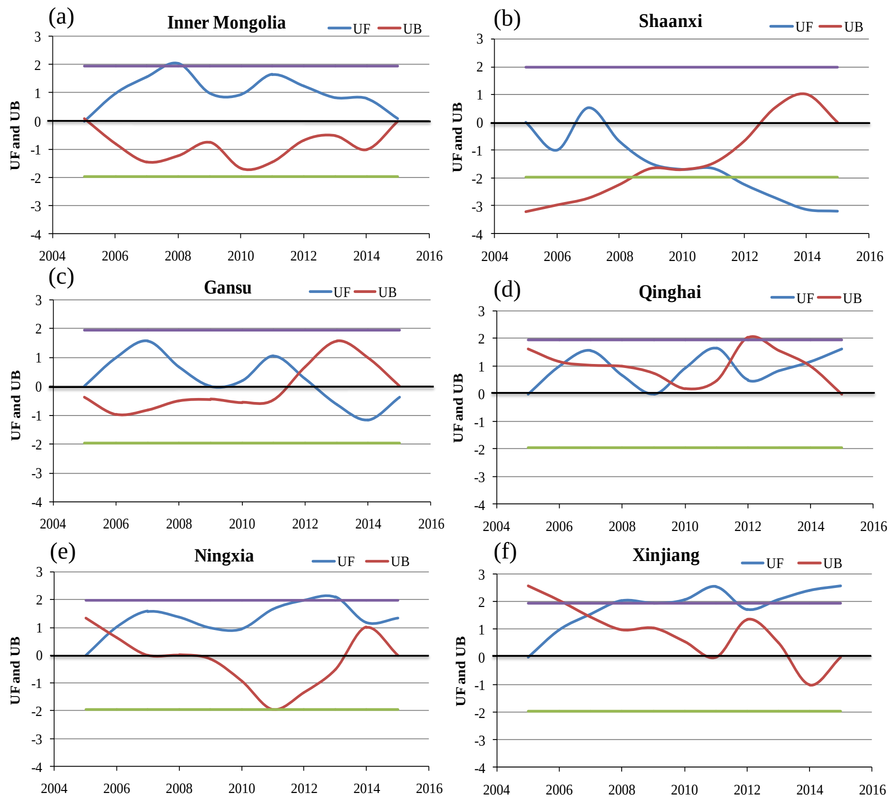

Figure 10

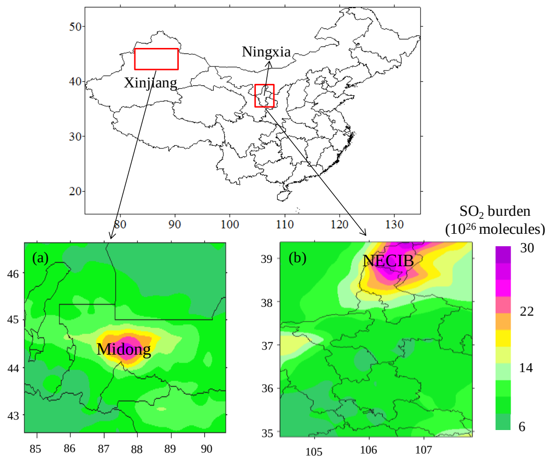

Figure 11